ISBN: 978-3-95450-216-5 doi:10.18429/JACoW-eeFACT2018-WEOAB04

SINGLE BUNCH INSTABILITIES AND NEG COATING FOR FCC-ee

E. Belli*, P. Costa Pinto, G. Rumolo, A. Sapountzis, T. Sinkovits, M. Taborelli,
CERN, Geneva, Switzerland
G. Castorina, M. Migliorati, University of Rome La Sapienza and INFN Sez.Roma1, Rome, Italy
B. Spataro, M. Zobov, INFN/LNF, Frascati (Rome)

Abstract

The high luminosity electron-positron collider FCC-ee is part of the Future Circular Collider (FCC) study at CERN and it has been designed to cover the beam energy range from 45.6 GeV to 182.5 GeV to study the properties of the Higgs boson and other particles. Electron cloud build up simulations on the Z resonance revealed the necessity of minimising the Secondary Electron Yield (SEY) of the pipe walls by applying a Ti-Zr-V Non-Evaporable Getter (NEG) coating in the entire ring. Beam dynamics simulations at 45.6 GeV pointed out that minimising the thickness of this layer is mandatory to reduce the resistive wall (RW) impedance, thus increasing the single bunch instability thresholds and ensuring beam stability during operation. However, reducing the coating thickness can affect the performance of the material and therefore the SEY. For this reason, an extensive measurement campaign was performed at CERN to characterise NEG thin films with thicknesses below 250 nm in terms of activation performance and SEY measurements. This paper also presents the FCC-ee longitudinal impedance model which includes all the current machine components.

INTRODUCTION

In 2014, CERN launched the Future Circular Collider (FCC) study [1] for the design of different circular colliders for the post-LHC era. This study is investigating a high energy proton-proton machine (FCC-hh) to reach a centre-of-mass energy of 100 TeV and a high luminosity electron-positron collider (FCC-ee) as a potential first step to cover a beam energy range from 45.6 GeV to 182.5 GeV, thus allowing to study the properties of the Higgs, W and Z bosons and top quark pair production thresholds with unprecedented precision. Table 1 summarizes the main beam parameters on the Z resonance which represents the most challenging scenario from the beam stability point of view.

Due to the beam parameters and pipe dimensions, electron cloud (EC) and collective effects due to the electromagnetic fields generated by the interaction of the beam with the vacuum chamber can be very critical aspects for the machine by producing instabilities that can limit its operation and performance.

This paper will present an estimation of the EC build up in the main magnets of the positron ring, the contributions of specific vacuum chamber components to the total impedance budget and their effects on single bunch beam dynamics. Special attention has been given to the resistive wall (RW) impedance, whose value is increased by a layer of Non-Evaporable Getter (NEG) coating which is required to reduce the Secondary Electron Yield (SEY) of the pipe walls for electron cloud mitigation [2, 3]. The studies presented in this paper will show that for the proposed lepton collider at 45.6 GeV the single bunch instability thresholds can be increased by decreasing the coating thickness. For this reason, in parallel to these numerical studies, an extensive measurement campaign was performed at CERN to investigate NEG thin films with thicknesses below 250 nm in terms of activation performance and SEY measurements, with the final purpose of finding the minimum effective thickness satisfying impedance, vacuum and electron cloud requirements.

Besides the RW, other impedance sources have been analyzed and the longitudinal impedance model thus obtained has been used to study the microwave instability and to predict its effects on the stability of the beam.

Table 1: FCC-ee baseline beam parameters at Z running. SR and BS stand for synchrotron radiation and beamstrahlung.

Beam energy [GeV]	**45.6**
Circumference C [km]	97.75
Number of bunches/beam	16640
Bunch population N_p [10^{11}]	1.7
Beam current I [A]	1.39
RF frequency f_{RF} [MHz]	400
RF voltage V_{RF} [MV]	100
Energy loss per turn [GeV]	0.036
Momentum compaction α_c[10^{-5}]	1.48
Bunch length $\sigma_{z,SR}/\sigma_{z,BS}$ [mm]	3.5/12.1
Energy spread $\sigma_{dp,SR}/\sigma_{dp,BS}$ [%]	0.038/0.132
Horizontal tune Q_x	269.138
Vertical tune Q_y	269.22
Synchrotron tune Q_s	0.025
Horizontal emittance ϵ_x [nm]	0.27
Vertical emittance ϵ_y [pm]	1.0

ELECTRON CLOUD STUDIES

This section presents EC build up studies in the positron ring of the lepton collider at 45.6 GeV. Build up simulations have been performed in the drift space and in all the magnets of the machine (dipoles and quadrupoles in the arcs and final focusing quadrupoles in the interaction region) by using the PyECLOUD [4, 5] code.

The bunch parameters used for simulations are listed in Table 1 while Table 2 summarizes the magnetic parameters of each element. For the beam optics in the arcs and around the interaction point, one can refer to [6]. In the arcs, the

* eleonora.belli@cern.ch

ISBN: 978-3-95450-216-5 doi:10.18429/JACoW-eeFACT2018-WEOAB04

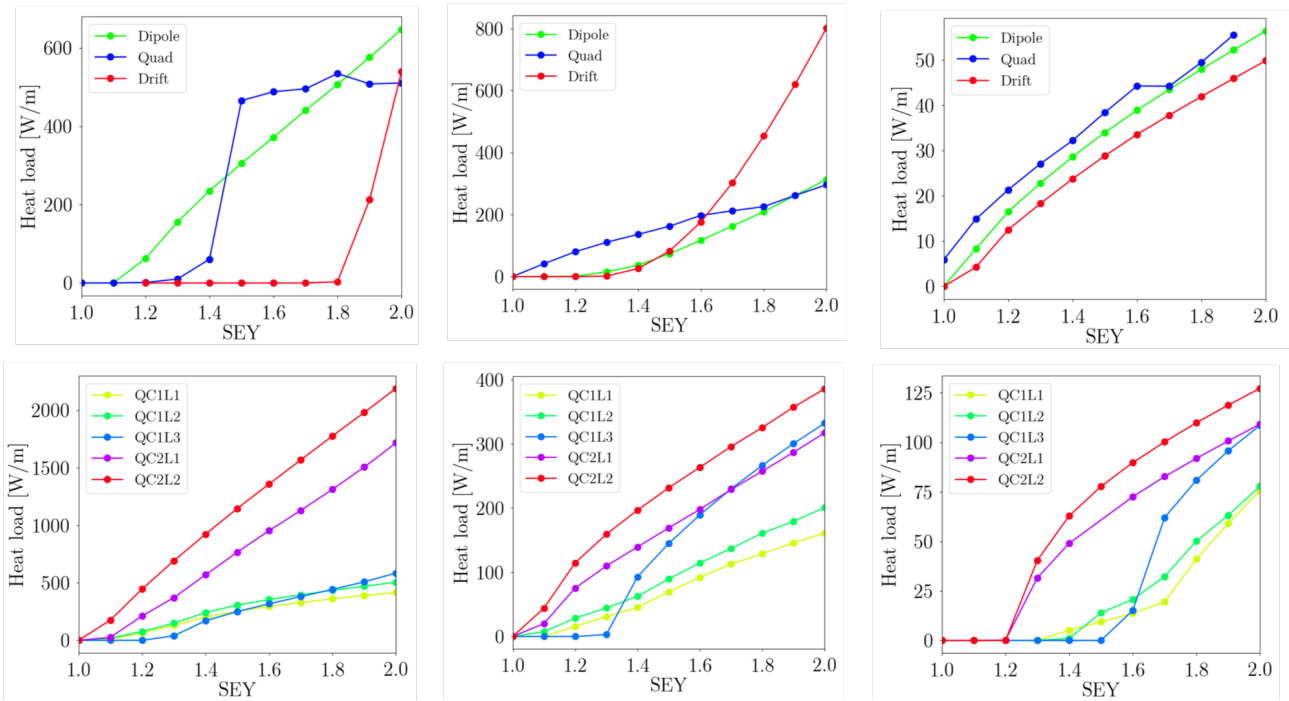

Figure 1: Heat load as a function of SEY for arc components (top) and IR magnets (bottom) in the case of 2.5 ns (left side), 5 ns (center) and 15 ns (right side) bunch spacings.

Table 2: Magnet parameters used for EC build up simulations at 45.6 GeV

Element	Length [m]	Magnetic field
Arc dipole	23.44	0.01415 T
Arc quadrupole	3.1	± 5.65 T/m
Arc drift	-	-
QC1L1	1.2	-96.3 T/m
QC1L2	1.0	50.3 T/m
QC1L3	1.0	9.8 T/m
QC2L1	1.25	6.7 T/m
QC2L2	1.25	3.2 T/m

Table 3: Threshold SEY for multipacting for all the ring components

Element	2.5 ns	5 ns	15 ns
Dipole	1.1	1.1	1.0
Quadrupole	1.2	1.0	<1.0
Drift	1.8	1.3	1.0
QC1L1	1.0	1.1	1.3
QC1L2	1.0	1.0	1.4
QC1L3	1.2	1.3	1.5
QC2L1	1.0	1.0	1.2
QC2L2	1.0	1.0	1.2

vacuum chamber is modelled as a circular pipe with 35 mm radius and two rectangular antechambers on both sides for the installation of synchrotron radiation absorbers, while in the final focusing quadrupoles of the interaction region (IR) the beam pipe is circular with 15 mm radius for the QC1 quadrupole and 20 mm radius for the QC2 quadrupole. According to RF computations [7], bunch spacing of 10 ns and 17.5 ns are not acceptable for the present cavity geometry and filling schemes with at least 100 RF buckets between the first bunches of consecutive trains are preferred. On the basis of these considerations, the EC build up in each element has been simulated by scanning the SEY for different bunch spacing of 2.5 ns, 5 ns and 15 ns and by assuming 4 trains of 80 bunches interleaved with 25 empty buckets at the nominal bunch intensity of $1.7 \cdot 10^{11}$ e^+/bunch. An initial uniform electron distribution of 10^9 e^-/m has been assumed in the vacuum chamber to model the survival of electrons between trains or between turns. The multipacting threshold, defined as the highest SEY without multipacting, has been evaluated for each element and beam and reported in Table 3: these results show that the highest thresholds of EC multipacting are given by the 2.5 ns beam in the arcs and by the 15 ns beam in the IR. Figure 1 shows the EC induced heat load as a function of SEY for different components and bunch spacings. Numerical simulations have also been performed including photoemission seeding [8, 9], showing that the heat load is not affected by photolectrons. Considering the beam parameters of Table 1, the analytic electron density threshold for the transverse instability [10] at low energy is about $2.29 \cdot 10^{10}/m^3$. Such a low threshold requires a low SEY coating in the entire ring, paying particular attention to the RW impedance seen by the beam.

ISBN: 978-3-95450-216-5 doi:10.18429/JACoW-eeFACT2018-WEOAB04

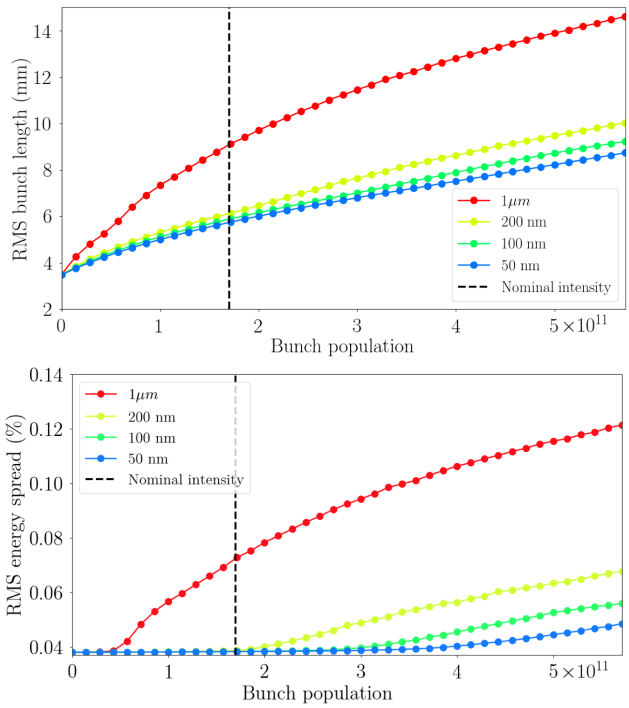

Figure 2: RMS bunch length (top) and RMS energy spread (bottom) as a function of the bunch population given by numerical simulations considering only the RW impedance produced by NEG films with different thicknesses. The dashed black line corresponds to the nominal bunch population.

RESISTIVE WALL IMPEDANCE

For RW impedance studies, the vacuum chamber is assumed to be circular with 35 mm radius and four layers: an outer layer of iron modelling the magnet chamber, then 6 mm of dielectric to consider the gap between the magnet chamber and the beam pipe, an inner layer of copper with 2 mm thickness and a NEG coating of the copper surface whose thickness has been investigated by means of numerical simulations in order to reduce the RW contribution. Analytical and numerical studies for FCC-ee at low energy [8, 9, 11] showed that the single bunch instability thresholds mainly depend on the thickness of the coating and only marginally on its conductivity. Moreover, the RW contribution can be decreased by reducing the film thickness. Simulations with the macroparticle tracking code PyHEADTAIL [12] have been performed considering NEG thin films with thicknesses of 1000 nm, 200 nm, 100 nm and 50 nm and the beam parameters of Table 1.

Microwave Instability

Figure 2 shows the bunch lengthening and the energy spread increase due to the longitudinal RW wakefield as a function of the bunch population for all the thicknesses under study. The instability threshold has been defined as the value of the bunch population corresponding to an increase of the energy spread of about 10% w.r.t. its nominal value. A standard coating of 1 μm thickness makes the bunch unstable in the longitudinal plane, while thinner films allow to significantly increase the microwave instability threshold. For example, in the case of 100 nm thickness the instability threshold is increased by a factor 7 with respect to 1 μm thickness and it is about 2 times higher than the nominal bunch intensity.

Transverse Mode Coupling Instability

The Transverse Mode Coupling Instability (TMCI) threshold has been evaluated with the analytical Vlasov solver DELPHI [13] by taking into account the bunch lengthening due to the longitudinal wake (Fig. 2). The instability threshold has been defined as the value of the bunch population where the frequencies of two neighboring modes are merging. In the transverse case, the instability threshold is affected to a lesser extent by the coating thickness, because the longitudinal wake produces longer bunches at higher intensities, which increases the TMCI threshold. As shown in Fig. 3, the TMCI threshold is about a factor 2.5 higher than the nominal bunch intensity for both 100 nm and 1μm thicknesses.

NEG THIN FILMS: EXPERIMENTAL CHARACTERIZATION

Reducing the thickness of NEG coatings for impedance requirements can affect the performance of the material itself and therefore the maximum SEY and related EC mitigation. In order to evaluate the activation performance and SEY, NEG films with thicknesses of 1000 nm, 200 nm, 100 nm and 50 nm were deposited on copper samples by DC magnetron sputtering [14]. More details about the coating process can be found in [8, 9]. The thickness was measured on cross sections of the samples and determined by Scanning Electron Microscopy (SEM) [15], resulting in film thicknesses of 1100 nm, 203 nm, 87 nm and 30 nm, obtained as average values from five measurements. Film composition was measured by energy dispersive X-ray spectroscopy to be 28 at.% Ti, 29 at.% Zr and 43 at.% V.

The surface composition and activation performance were measured by X-ray Photoelectron Spectroscopy (XPS) [16]. The multiplex spectra have been taken at four different steps:

- as received sample, at room temperature
- after 1h heating at 160°C
- after 1h heating at 200°C
- after 1h heating at 250°C

Four activation cycles were performed, with air exposure between two consecutive cycles. The activation performance was evaluated by the reduction of the area of the oxygen peak O1s after the fourth activation cycle. A higher reduction of the oxygen corresponds to a better activation and the results shown in Fig. 4 show that the oxygen surface concentration is increasing for thinner layers.

ISBN: 978-3-95450-216-5 doi:10.18429/JACoW-eeFACT2018-WEOAB04

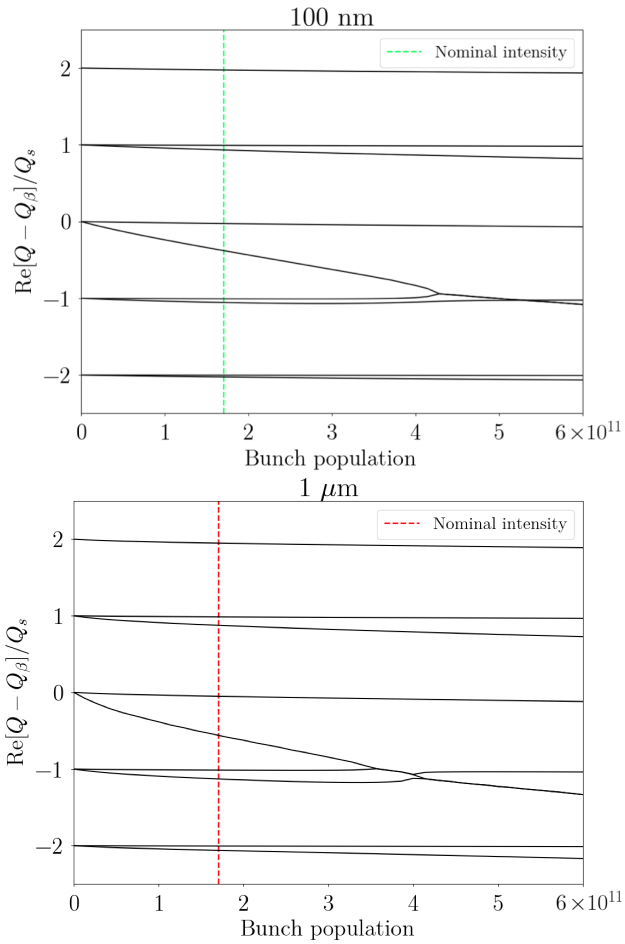

Figure 3: Real part of the tune shift of the first coherent oscillation modes as a function of the bunch population for 100 nm (top) and 1 μm (bottom) thicknesses. The dashed lines correspond to the nominal bunch population.

Figure 5 shows the oxidation state of the metals after the fourth activation cycle. One can observe mainly metallic components on Ti and V and a strong oxide component on Zr for the 87 nm and 30 nm films after activation.

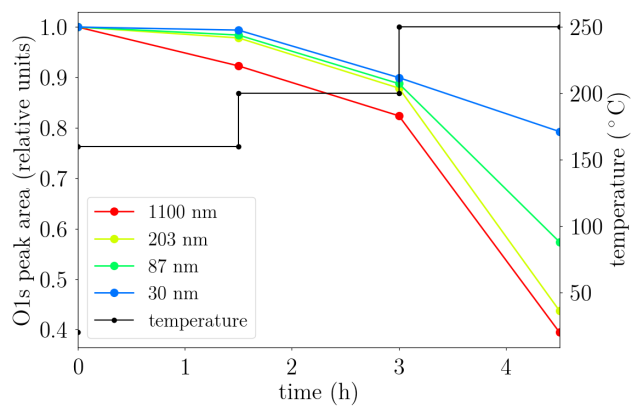

Figure 4: O1s peak area as a function of the activation time and temperature after the fourth activation cycle.

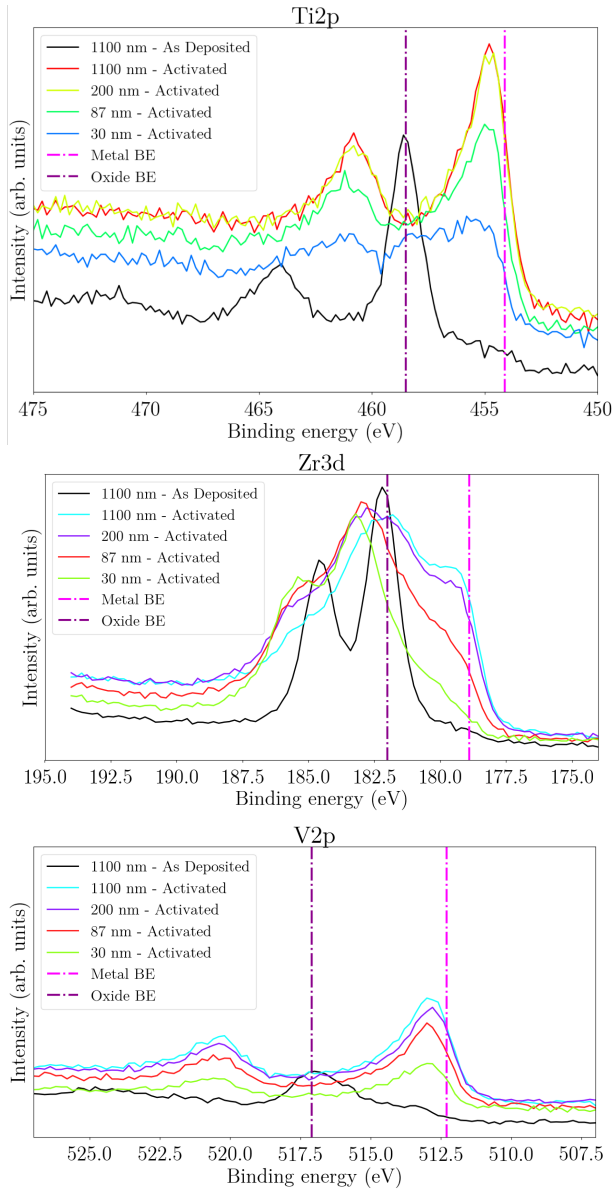

Figure 5: Ti2p (top), Zr3d (centre) and V2p (bottom) photopeaks obtained by XPS analysis for all the thicknesses under study. 2p and 3d refer to subshells of electronic configuration.

Figure 6 shows the depth profile for each sample after the fourth activation cycle. The oxygen content is decreasing rapidly in all films but while in the 1100 nm sample it decreases below 5% in less than 100 nm, in the thinner samples it is detected in the whole layer. In particular, in the 30 nm film the oxygen concentration goes from 50% at the surface to 30% inside the layer and this big loss in gradient represents the major limiting factor for the material activation, considering that the diffusion of oxygen from the surface oxide to the bulk of the material is faster in case of steep gradient.

SEY measurements were performed by using the experimental set-up described in [8, 9]. Figure 7 shows the SEY

ISBN: 978-3-95450-216-5 doi:10.18429/JACoW-eeFACT2018-WEOAB04

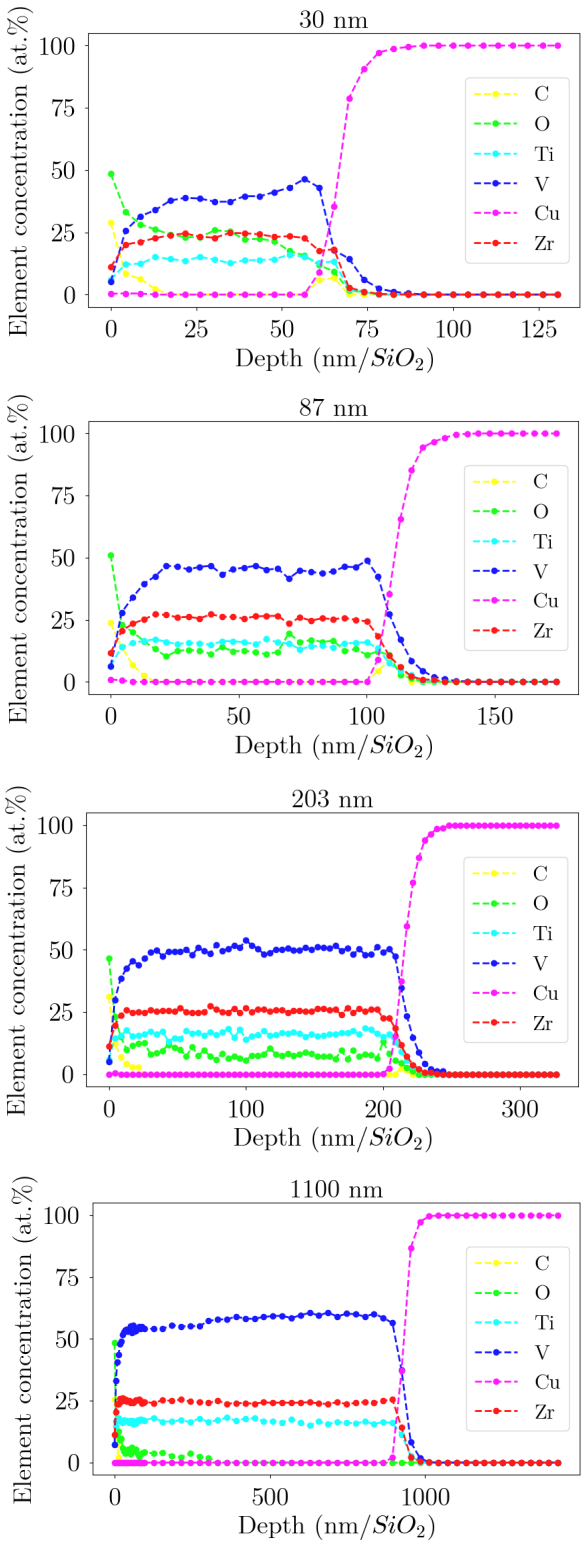

Figure 6: Profile of C, O, Ti, V, Zr and Cu as a function of depth for all the samples.

curves for all the samples under study after the fourth activation cycle, showing that the SEY is increasing for thinner layers. As shown in Fig. 8, elevated concentrations of oxygen in thinner films are responsible for higher SEY. SEY

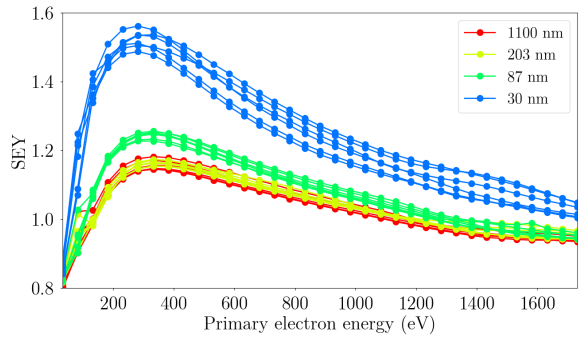

Figure 7: SEY as a function of photoelectrons energy for all the samples under study after the fourth activation cycle of 4 hours up to a temperature of 250°C.

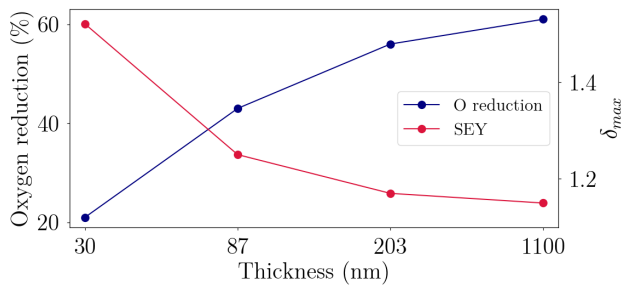

Figure 8: Oxygen reduction and maximum SEY as a function of the coating thickness for all the samples under study after the fourth activation cycle of 4 hours up to a temperature of 250°C.

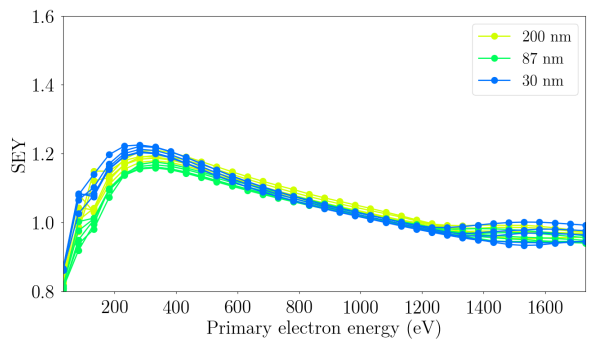

Figure 9: SEY as a function of photoelectrons energy for the thin films after the fourth activation cycle of 24 hours up to a temperature of 250°C.

measurements were also performed after longer activation cycles of 24 hours at the same temperature (see Fig. 9), showing a lower SEY compared to the one obtained after shorter activation times. For example, for the 87 nm sample the SEY was reduced from 1.25 to 1.16.

LONGITUDINAL IMPEDANCE MODEL

The FCC-ee impedance model includes all the current vacuum chamber components: RW (with 100 nm NEG film), vertical and horizontal collimators [17, 18], 400 MHz radio-frequency (RF) cavities [19, 20] with tapers, Beam

ISBN: 978-3-95450-216-5 doi:10.18429/JACoW-eeFACT2018-WEOAB04

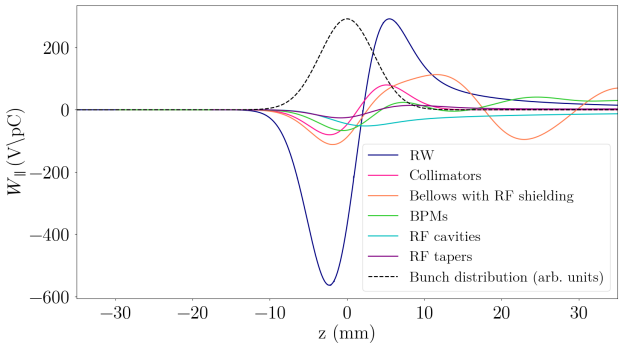

Figure 10: Longitudinal wake potentials for a Gaussian bunch with nominal bunch length σ_z = 3.5 mm due to the main FCC-ee components compared with the RW contribution (blue line).

Table 4: Power loss contribution of the main FCC-ee components at nominal intensity and bunch length, in the lowest energy case of 45.6 GeV

Component	**Number**	$k_{loss}[V/pC]$	$P_{loss}[MW]$
Resistive wall	97.75km	210	7.95
Collimators	20	18.7	0.7
RF cavities	56	18.5	0.7
Double tapers	14	26.6	1.0
BPMs	4000	40.1	1.5
Bellows	8000	49.0	1.8
Total		**362.9**	**13.7**

Position Monitors [21, 22] and bellows with RF shielding [23]. The contribution of these components to the longitudinal impedance budget has been evaluated by means of ABCI [24] and CST [25] simulations in time domain for a Gaussian bunch with nominal RMS bunch length of σ_z = 3.5 mm. Figure 10 shows the longitudinal wake potentials of each component while Table 4 summarizes the corresponding loss factors. The major contribution to the machine impedance is given by the RW with a total loss factor at nominal intensity and bunch length of 210 V/pC. The total dissipated power at nominal intensity is 13.6 MW, about a factor 3.6 smaller than the total SR power dissipated by the beam of 50 MW. However, this value of power loss is expected to be lower due to the bunch lenghtening effect. From Fig. 11, one can observe that at nominal intensity the bunch length increases of only 7% in case of beamstrahlung while without beamstrahlung the bunch length is twice the nominal value. The MI threshold is about $2.5 \cdot 10^{11}$, a factor of 1.5 larger than the nominal bunch intensity, and is much higher with beamstrahlung.

CONCLUSIONS

This paper analyses the main limitations for the operation of the lepton collider FCC-ee, i.e. EC and collective effects, particularly critical on the Z resonance due to the low energy and the high beam current. EC build up simulations

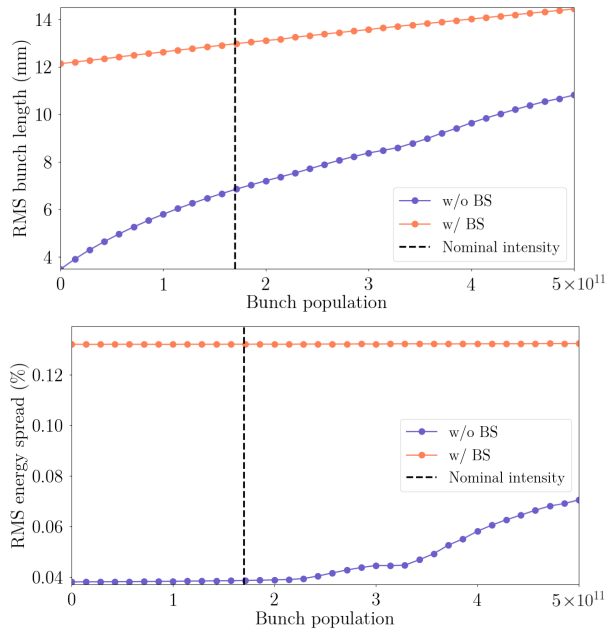

Figure 11: RMS bunch length (top) and RMS energy spread (bottom) as a function of the bunch population given by numerical simulations by considering the impedance contribution of all the machine components. The black dashed line represents the nominal bunch intensity.

have been performed for the main elements of the positron ring, in both the arcs and the IR. Multipacting thresholds and heat load have been evaluated for each component for different bunch spacings of 2.5, 5, 15 ns, indicating that with a low SEY coating (SEY ≤ 1.2) the 15 ns beam is the preferable option to suppress the EC build up in the IR and to have a lower heat load in the arcs. This coating is also needed to cope with the EC induced single bunch head tail instability, whose electron density threshold on the Z resonance is quite low (about $2.29 \cdot 10^{10}/m^3$). An impedance model was also developed, with special attention to the RW impedance representing the main source of wakefields in the machine. Numerical studies showed that its contribution to the impedance budget can be reduced by decreasing the thickness of NEG coating needed for vacuum requirements and electron cloud mitigation. The minimum effective thickness for NEG activation was examined using XPS. Elevated concentrations of oxygen especially in the thinner films are responsible for reduced activation performance. After four short activation cycles of 4 hours, the thinnest sample of 30 nm was unable to activate effectively and this led to a high maximum SEY of 1.5. Longer activation cycles of 24 hours led to better activation and a lower SEY of 1.21 after the fourth cycle. Numerical simulations and experimental results indicated that a film thickness between 100 nm and 200 nm balancing the limitations of activation and impedance is a good candidate for coating thickness. Further experimental investigation is recommended for SEY and photon-stimulated desorption with a larger number of activation cycles. The impedance has been evaluated for

ISBN: 978-3-95450-216-5 doi:10.18429/JACoW-eeFACT2018-WEOAB04

important machine components, showing that the contribution of these elements is up to 5 times smaller than that of RW. The MI threshold is around $2.5 \cdot 10^{11}$, about a factor 1.5 higher than the nominal bunch intensity. Operation with beamstrahlung will increase the instability thresholds in both planes.

ACKNOWLEDGEMENTS

The authors would like to thank D. Letant-Delrieux, H. Neupert, K. Oide, V. Petit, F. Zimmermann for their help and for the very useful discussions. This work was supported in part by the European Commission under the HORIZON 2020 Integrating Activity project ARIES, Grant Agreement No. 730871.

REFERENCES

[1] https://fcc.web.cern.ch

[2] P.C. Pinto, S. Calatroni, P. Chiggiato, H. Neupert, W. Vollenberg, E. Shaposhnikova, M. Taborelli, and C.Y. Vallgren, Thin film coatings for suppressing electron multipacting in particle accelerators, in *Proceedings of the 2011 Particle Accelerator Conference*, New York, NY (2011), pp. 2096-2098, https://cds.cern.ch/record/1462768.

[3] P.C. Pinto, History and potential of Non Evaporable Getter (NEG) technology, in *Workshop on Advanced Materials and Surfaces, CERN, Geneva, Switzerland* (2013), https://indico.cern.ch/event/229108/contributions/1539894/.

[4] https://github.com/PyCOMPLETE/PyECLOUD

[5] G. Iadarola, Electron cloud studies for CERN particle accelerators and simulation code development, CERN Report No. CERN-THESIS-2014-047 (2014).

[6] K. Oide, Status of optics, in *Proceedings FCC Week 2017 - 31 May 2017, Berlin, Germany*, https://indico.cern.ch/event/556692/contributions/2590161/.

[7] I. Karpov, R. Calaga, and E.Chapochnikova, High order mode power loss evaluation in future circular electron-positron collider cavities, *Phys. Rev. Accel. Beams* vol. 21, p. 071001 (2018).

[8] E. Belli, et al., Electron cloud buildup and impedance effects on beam dynamics in the Future Circular e^+e^- Collider and experimental characterization of thin TiZrV vacuum chamber coatings, *Phys. Rev. Accel. Beams*, accepted for publication (2018).

[9] E. Belli, Coupling impedance and single beam collective effects for the Future Circular Collider (lepton option), Ph.D. Thesis, to be published.

[10] K. Ohmi, Study of electron cloud effects in SuperKEKB, in *Proceedings of IPAC'14*, Dresden, Germany (2014), pp. 1597-1599.

[11] M. Migliorati, E. Belli, and M. Zobov, Impact of the resistive wall impedance on beam dynamics in the Future Circular e+e- Collider, *Phys. Rev. Accel. Beams* vol. 21, p. 041001 (2018).

[12] https://github.com/PyCOMPLETE/PyHEADTAIL

[13] https://twiki.cern.ch/twiki/bin/view/ABPComputing/DELPHI

[14] P. Chiggiato, P. Costa Pinto, Ti-Zr-V non-evaporable getter films: from development to large scale production for the Large Hadron Collider, in *Thin Solid Films* vol. 515, pp. 382-388 (2006).

[15] http://en-dep.web.cern.ch/en-dep/Groups/MME/MM/SEM.htm

[16] J. F. Moulder, et al., Handbook of X-ray Photoelectron Spectroscopy, Perkin-Elmer Corporation, Physical Electronics Division, 1992.

[17] S. DeBarger, et al., The PEP-II movable collimators, No. SLAC-PUB-11752 (2001).

[18] T. Ishibashi, Low impedance movable collimators for SuperKEKB, in *Proceedings of IPAC'17*, Copenhagen, Denmark (2017), pp. 14-19.

[19] A. Butterworth, Cavity design and beam-cavity interaction challenges, in *Proceedings FCC Week 2017 - 30 May 2017, Berlin, Germany*, https://indico.cern.ch/event/556692/contributions/2484361/.

[20] S.G. Zadeh, Cavity design approaches and HOM damping for FCC-ee, in *Proceedings FCC Week 2017 - 30 May 2017, Berlin, Germany*, https://indico.cern.ch/event/556692/contributions/2484333/.

[21] F. Marcellini, M. Serio, A. Stella, and M. Zobov, DAPHNE broad-band button electrodes, in *Nucl. Instrum. Meth. A* vol. 402, pp. 27-35 (1998).

[22] A. Rodrigues, et al., Sirius status report, in *Proceedings of IPAC'16, Busan*, Korea (2016), pp. 2811-2814.

[23] Y. Suetsugu, M. Shirai, and K. Shibata. Possibility of comb-type rf shield structure for high-current accelerators, *Phys. Rev. ST Accel. Beams* vol. 6, p. 103201 (2003).

[24] http://abci.kek.jp/

[25] https://www.cst.com